Synthesis and magnetic properties of nickel three-dimensional superlattice structure

Hongyan Duan, Fagen Li, Wei Wu, Jun Wang

Faculty of Science, Ningbo University, Ningbo, People's Republic of China
E-mail: wjnaf@ustc.edu

Published in Micro & Nano Letters; Received on 12th December 2012; Revised on 13th March 2013; Accepted on 4th April 2013

High monodisperse nickel nanoparticles of 13 nm were successfully synthesised based on reduction of common nickel salts. Further annealing process prompted the formation of magnetic superlattices. The morphological features characterised by field emission scanning electron microscopy showed that the Ni nanoparticles self-assembled periodically and formed close-packed arrays. The results of magnetic hysteresis loops showed that the sample exhibited improved magnetic properties compared with those of other bigger nanoparticles. The Curie temperature of the sample was about 596 K, lower than that of the bulk material, which is discussed in terms of the finite-size effects.

1. Introduction: Nanomagnetic materials have been the focus for decades owing to their promising applied advantages in data storage media, magnetic fluid, sensors and drug targeting carriers [1–4]. Magnetic nanoparticles with controllable particle size have attracted more attention because of the dependence of their physical properties on their sizes. Many methods have been attempted for synthesis of magnetic nanoparticles, such as polyol synthesis, the sol–gel technique and electrochemical reductions [5–8]. Up to now, particles with broad size distributions, from 2 nm to bulk stage, have been synthesised and assembled to various morphologies, including wire, sphere and core–shell structures [9–13]. In recent years, two- and three-dimensional (3D) superlattice structures built from self-organisation of nanoparticles have been conducted and successfully achieved in the cases of FePt, FeCo and Fe_3O_4 [14–16].

The superlattice structures were generally achieved through the procedure of size separation, spontaneously self-assembled on a surface or by layer-by-layer deposition [15]. The pre-prepared highly monodisperse nanoparticles are critical to the formation of the superlattice structures. Park *et al.* [4] synthesised highly monodisperse nickel nanoparticles and obtained nickel superlattice structure. Shevchenko *et al.* [17] developed a three-layer technique to obtain superlattices. The process is single, complicated and limited for large-scale production. It is essential to develop more methods for synthesising magnetic superlattices.

In our previous work, we have synthesised highly monodisperse magnetic nanoparticles with different size distribution [18–21]. Herein, we report a facile chemical method for controllable synthesis of nickel superlattices. The synthetic process was based on chemical reduction of common nickel salts $Ni(acac)_2$. The obtained dried powder was collected for further usage. We changed the surface properties of the nanoparticles through annealing treatment and obtained superlattices directly at the temperature of 300°C. The magnetic property of the nickel superlattices was investigated in detail. Our works may provide a new facile method for synthesising superlattice structures.

2. Experiment: In a typical procedure, 25 mg (7.80 mmol) [$Ni(acac)_2$] was added to the mixture of 25 ml (78.0 mmol) oleylamine and 3 ml (6.24 mmol) trioctylphosphine. Oleylamine acted as both the solvent and the reductant, affecting the rate of nucleation. The solution was heated to 100°C in a two-neck round-bottom flask under an argon atmosphere. Then the temperature rose to 220°C quickly and remained there for 60 min. The obtained black solid product was separated from the solution by magnetic separation, and then washed with ethanol and n-hexane several times. The sample was dried in a vacuum at 60°C for 6 h. Finally, the dried particles were annealed at 300°C for 2 h under an argon atmosphere. The obtained sample was collected for further usage.

Structure characterisation of the sample was performed by means of X-ray diffraction (XRD) using a diffractometer (D/Max-γA) with CuKα radiation ($\lambda = 1.5418$ Å). The data were collected in the range of 20–90 (2θ). The morphology and elements of the sample were measured by a scanning electron microscope (FE-SEM SU-70) with energy-dispersive X-ray (EDX). Transmission electron microscopy (TEM) and high-resolution transmission electron microscopy (HRTEM) measurements were performed on FEI Tecnai F20. Magnetic measurements were performed using a Quantum Design vibrating sample magnetometer.

3. Results and discussion: Fig. 1*a* shows the HRTEM image of the synthesised nickel nanoparticles and the inset of Fig. 1*a* further demonstrates that the particles display a lattice spacing of 0.208 nm, consistent with the (111) crystal plane of nickel. The TEM image in Fig. 1*b* clearly indicates that the products are uniform with narrow size distributions and particle sizes of 13 nm, agreeing with this result of the histogram of size distributions in Fig. 1*c*.

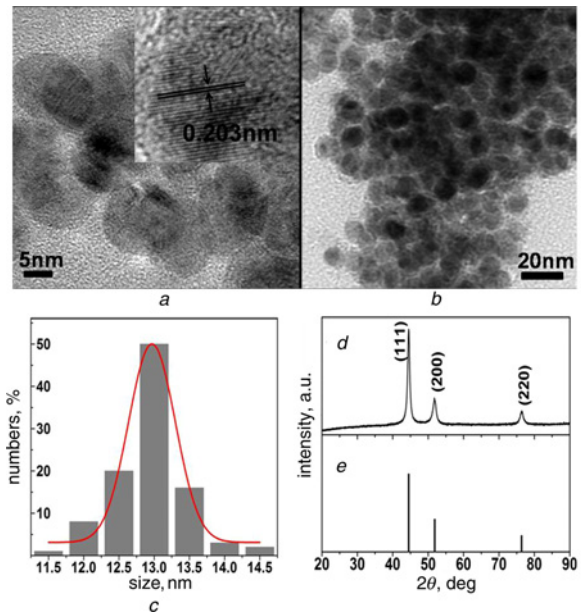

Figure 1 *HRTEM image of the synthesised nickel nanoparticles (Fig. 1a) (inset shows the lattice fringe image); TEM image of nanoparticles with size of about 13 nm (Fig. 1b); histogram of particles size distribution (Fig. 1c); XRD pattern of as-prepared sample (Fig. 1d); XRD patterns of JCPDS Card No. 04-0850 (Fig. 1e)*

© The Institution of Engineering and Technology 2013

doi: 10.1049/mnl.2012.0945

The XRD pattern in Fig. 1*d* verifies the crystallinity and composition of the products. All the diffraction peaks can be indexed as the standard face-centred-cubic nickel structure with the lattice constant of 3.528 ± 0.004 Å, which is consistent with the values in the standard card (JCPDS No. 04-0850, Fig. 1*e*). The particle size calculated using the Debye-Scherrer formula from the reflection peak of (111) is about 13 nm, close to the determined result from the TEM and SEM images.

The SEM images of the as-prepared sample show a typical 3D superlattice structure (Figs. 2*a* and *b*). Compared with the SEM image of the particles before thermal treatment (Fig. 2*d*), we find that the nickel nanoparticles of thermal treatment display a superlattice structure, which indicates that the annealing process is significant for the formation of the superlattice structure. The evolution process can be described as follows. Under a high-temperature condition, the tendency of the solid phase in the systems prompted the recrystallisation of the smaller particles to achieve a minimum total surface energy [22]. However, the existence of the surfactant restrained the process of recrystallisation. The thermal treatment process could only prompt the interaction of the surfactant. As a result, the high-monodispersed nanoparticles formed a superlattice structure and the particles were linked by a weak hydrogen bond, Van der Waals force and electric/magnetic dipole interactions [14]. In the EDX spectra (Fig. 2*c*), the obtained elemental signatures were identical within experimental accuracy. The slight peaks of C, Ag, Al and P were caused by the silver conductive adhesive substrate (C, Ag), the Al sample stage and the reactant TOP (P), respectively.

Fig. 3*a* displays the magnetic hysteresis loops at 4 and 300 K for the sample. At 300 K, the coercivity H_C is about 50 Oe, higher than that of bulk nickel (0.7 Oe). Although the saturation magnetisation M_S reaches 18 emu/g, lower than the value of bulk nickel (55 emu/g) [23], these phenomena can be caused by typical surface properties of the nanoparticles. The surfaces of nanoparticles usually exhibit some degree of spin disorder and pinning. However, the M_S value of the obtained sample is higher than that of the 30 nm nanoparticles synthesised through direct metal reduction (10 emu/g) [24]. Fig. 3*b* displays a comparison of magnetic hysteresis loops at 300 K for the superlattices and the original particles without annealing treatment. Both the MS values and the HC values of the obtained sample are higher than the value of the original particles (14 emu/g, 30 Oe). The enhancement of the magnetic properties can contribute to improved crystallinity resulting from the annealing treatment.

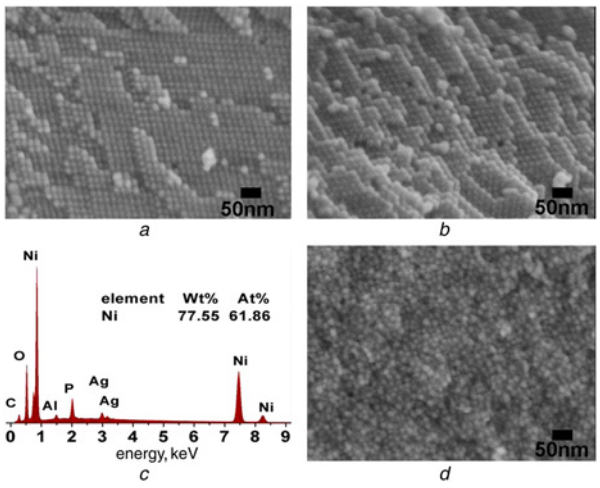

Figure 2 *Level surface image of typical self-assembled 3D superlattices (Fig. 2a); fracture surface image of superlattices (Fig. 2b); EDX spectra of sample (Fig. 2c); image of particles before annealing treatment (Fig. 2d)*

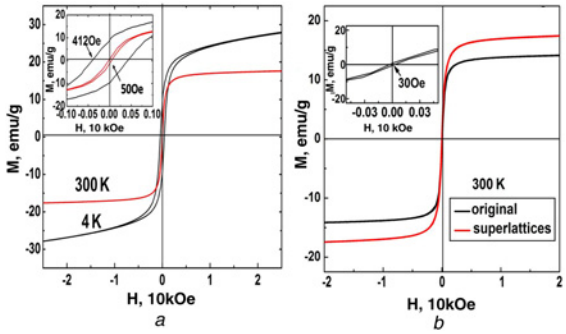

Figure 3 *Magnetic hysteresis loops at 4 and 300 K for sample (Fig. 3a) (inset is enlarged magnetisation curve of sample); magnetic hysteresis loops at 300 K for samples before and after annealing treatment (Fig. 3b) (inset is enlarged magnetisation curve of original sample before annealing treatment)*

The M_S and H_C values of the sample at 4 K (28 emu/g, 412 Oe) are higher than those of the particles at 300 K (18 emu/g, 50 Oe). This phenomenon can be explained by the theory of low temperature spin wave [13, 25]. The temperature dependence of the magnetisation between 4 and 300 K could be fitted to spin-wave-type dependence

$$M_S(T) = M_S(0)\left(1 - \beta T^b\right)$$

where $M_S(0)$, β and b are the saturation magnetisation at 0 K, the Bloch constant and the Bloch exponent, respectively. Therefore the value of M_S decreases with temperature increasing. The coercivity of the nanoparticles at low temperature follows the equation

$$H_C = \pm 2K_1/(\mu_0 M_S)$$

where K_1 and μ_0 are the magnetocrystalline anisotropy constant and vacuum susceptibility, respectively. It is obvious that the magnetocrystalline anisotropy constant decreases with increasing temperature, hence the coercivity increases rapidly at 4 K.

The high-temperature magnetic properties of the nickel nanoparticles were also studied. Fig. 4*a* plots the temperature dependencies of the warm-up and cool-down magnetisations for the sample measured in an applied field of 10 kOe. It is obvious that cool-down magnetisation at each temperature is higher than warm-up magnetisation. Large enhancement in magnetisation during the cooling procedure should be caused by significant growth of particle size at high temperature. For the warm-up curve, no visible upturn in magnetisation was observed before the Curie temperature was reached. The results suggest that the size growth does not occur before the Curie temperature is reached and the warm-up data are corresponding to the given particle size. To see the magnetic transitions more clearly, we plotted the reciprocal of the susceptibility (1/

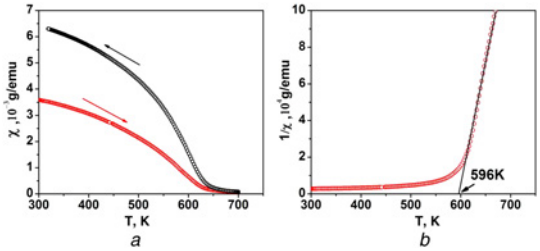

Figure 4 *Temperature dependencies of warm-up and cool-down magnetisations for sample (Fig. 4a); reciprocal of susceptibility (1/χ) against temperature (Fig. 4b) (susceptibility above Curie temperature is fitted by Curie-Weiss law (solid lines): $\chi = C/(T - T_C)$; T_C is indicated by arrows)*

© The Institution of Engineering and Technology 2013

χ, warm-up curve) against temperature of the sample (Fig. 4*b*). The susceptibility above the Curie temperature is fitted by the Curie-Weiss law (solid lines)

$$\chi = C/(T - T_C)$$

The intercept of the solid line on the temperature axes should correspond to the Curie temperature (T_C), about 596 K, lower than that of face-centred-cubic nickel bulk (627 K). The Curie temperatures of magnetic nanoparticles decrease with decreasing particle size, caused by finite-size effects [26].

4. Conclusions: We have successfully synthesised monodisperse nickel nanoparticles and obtained a superlattice structure via annealing processing. The mean diameter of the nanoparticles was about 13 nm. At 300 K, the sample displayed enhanced saturation magnetisation than that of bigger nanoparticles. The improved magnetic property could be a result of the annealing treatment process improving the crystallinity of the sample. The magnetic hysteresis loops at 4 and 300 K showed a typical feature of the theory of low temperature spin wave. The high-temperature magnetic property of the superlattices showed that the Curie temperature was lower than the value of bulk nickel, following the finite-size scaling relation.

5. Acknowledgments: This work was supported by the National Natural Science Foundation of China (11174165), the Natural Science Foundation of Ningbo (2012A610051) and the K. C. Wong Magna Foundation.

6 References

[1] Gotoh A., Uchida H., Ishizaki M., *ET AL.*: 'Simple synthesis of three primary colour nanoparticle inks of Prussian blue and its analogues', *Nanotechnology*, 2007, **18**, pp. 345609(1)–345609(6)

[2] Lee J.H., Huh Y.M., Jun Y., *ET AL.*: 'Artificially engineered magnetic nanoparticles for ultra-sensitive molecular imaging', *Nat. Med*., 2006, **13**, pp. 95–99

[3] Maeng J.H., Lee D.H., Jung K.H., *ET AL.*: 'Multifunctional doxorubicin loaded superparamagnetic iron oxide nanoparticles for chemotherapy and magnetic resonance imaging in liver cancer', *Biomaterials*, 2010, **31**, pp. 4995–5006

[4] Park J., Kang E., Son S.U., *ET AL.*: 'Monodisperse nanoparticles of Ni and NiO: synthesis, characterization, self-assembled superlattices and catalytic coupling reaction', *Adv. Mater*., 2005, **17**, pp. 429–434

[5] Hinotsu T., Jeyadevan B., Chinnasamy C.N., Shinoda K., Tohji K.: 'Size and structure control of magnetic nanoparticles by using a modified polyol process', *J. Appl. Phys*., 2004, **95**, pp. 7477–7479

[6] Chatterjee A., Chakravorty D.: 'Preparation of nickel nanoparticles by metalorganic route', *Appl. Phys. Lett*., 1992, **60**, pp. 138–140

[7] Sun Y.P., Rollins H.W., Guduru R.: 'Preparations of nickel, cobalt, and iron nanoparticles through the rapid expansion of supercritical fluid solutions and chemical reduction', *Chem. Mater*., 1999, **11**, pp. 7–9

[8] Han M., Liu Q., He J.H., Song Y., Xu Z., Zhu J.M.: 'Controllable synthesis and magnetic properties of cubic and hexagonal phase nickel nanocrystals', *Adv. Mater*., 2007, **19**, pp. 1096–1100

[9] Lee I.I.S., Lee N., Park J., *ET AL.*: 'Ni/NiO core/shell nanoparticles for selective binding and magnetic separation of histidine-tagged proteins', *J. Am. Chem. Soc.*, 2006, **128**, pp. 10658–10659

[10] Suber L., Imperatori P., Ausanio G., Fabbri F., Hofmeister H.: 'Synthesis, morphology and magnetic characterization of iron oxide nanowires and nanotubes', *J. Phys. Chem. B*, 2005, **109**, pp. 7103–7109

[11] Kim J., Lee J.E., Lee S.H., *ET AL.*: 'Designed fabrication of a multifunctional polymer nanomedical platform for simultaneous cancer-targeted imaging and magnetically guided drug delivery', *Adv. Mater*., 2008, **20**, pp. 478–483

[12] Cordente N., Respaud M., Senocq F., Casanove M.J.: 'Synthesis and magnetic properties of nickel nanorods', *Nano Lett*., 2001, **1**, pp. 565–568

[13] Zhao L.J., Zhang H.J., Xing Y., *ET AL.*: 'morphology-controlled synthesis of magnetites with nanoporous structures and excellent magnetic properties', *Chem. Mater*., 2008, **20**, pp. 198–204

[14] Sun S.: 'Recent advances in chemical synthesis, self-assembly, and applications of FePt nanoparticles', *Adv. Mater*., 2006, **18**, pp. 393–403

[15] Desvaux C., Amiens C., Fejes P., Renaud P.: 'Multimillimetre-large superlattices of air-stable iron–cobalt nanoparticles', *Nat. Mater.*, 2005, **4**, pp. 750–753

[16] Zhang L., Wu J., Liao H., Hou Y., Gao S.: 'Octahedral Fe_3O_4 nanoparticles and their assembled structures', *Chem. Commun*., 2009, **29**, pp. 4378–4380

[17] Shevchenko E., Talapin D., Kornowski A., *ET AL.*: 'Colloidal crystals of monodisperse FePt nanoparticles grown by a three-layer technique of controlled oversaturation', Advanced Materials, 2002, **14**, pp. 287–290

[18] Wang J., Wu W., Zhao F., Zhao G.M.: 'Curie temperature reduction in SiO_2-coated ultrafine Fe_3O_4 nanoparticles: quantitative agreement with a finite-size scaling law', *Appl. Phys. Lett*., 2011, **98**, pp. 083107 (1)–083107(3)

[19] Wang J., Zhao F., Wu W., Cao S., Zhao G.M.: 'Magnetic properties in silica-coated $CoFe_2O_4$ nanoparticles: quantitative test for a theory of single-domain particles with cubic anisotropy', *Phys. Lett. A*, 2012, **376**, pp. 547–549

[20] Wang J., Zhao F., Wu W., Zhao G.M.: 'Finite-size scaling relation of the Curie temperature in barium hexaferrite platelets', *J. Appl. Phys*., 2011, **110**, pp. 123909(1)–123909(3)

[21] Wang J., Wu W., Zhao F., Zhao G.M.: 'Suppression of the Neel temperature in hydrothermally synthesized α-Fe_2O_3 nanoparticles', *J. Appl. Phys*., 2011, **109**, pp. 056101(1)–056101(3)

[22] Shen J., Zhao Z., Peng H., Nygren M.: 'Formation of tough interlocking microstructures in silicon nitride ceramics by dynamic ripening', *Nature*, 2002, **417**, pp. 266–269

[23] Hou Y., Gao S.: 'Monodisperse nickel nanoparticles prepared from a monosurfactant system and their magnetic properties', *J. Mater. Chem*., 2003, **13**, pp. 1510–1512

[24] Sidhaye D.S., Bala T., Srinath S., *ET AL.*: 'Preparation of nearly monodisperse nickel nanoparticles by a facile solution based methodology and their ordered assemblies', *J. Phys. Chem. C*, 2009, **113**, pp. 3426–3429

[25] Mori H., Kawasaki K.: 'Theory of dynamical behaviors of ferromagnetic spins', *Prog. Theory Phys*., 1962, **27**, pp. 529–570

[26] Fisher M.E., Ferdinand A.E.: 'Interfacial, boundary, and size effects at critical points', *Phys. Rev. Lett*., 1967, **19**, pp. 169–172

© The Institution of Engineering and Technology 2013

doi: 10.1049/mnl.2012.0945